

Electronic Supplementary Material (ESI) for Dalton Transactions.
This journal is © The Royal Society of Chemistry 2020

Electronic Supplementary Material (ESI) for

Structural and magnetic studies of mononuclear lanthanide complexes derived from N-rich chiral Schiff bases.

E. Pilichos,^a M. Font-Bardia,^b A. Escuer,^{*a} and J. Mayans^{*c}

^a Departament de Química Inorgànica i Orgànica, Secció Inorgànica and Institute of Nanoscience (IN²UB) and Nanotechnology, Universitat de Barcelona, Martí i Franquès 1-11, Barcelona-08028, Spain.

^b Departament de Mineralogia, Cristal·lografia i Dipòsits Minerals and Unitat de Difracció de R-X. Centre Científic i Tecnològic de la Universitat de Barcelona (CCiTUB). Universitat de Barcelona. Solé i Sabarís 1-3. 08028 Barcelona.

^c Instituto de Ciencia Molecular (ICMol), Universidad de Valencia, Catedrático José Beltran 2, 46980 Paterna (Valencia), Spain

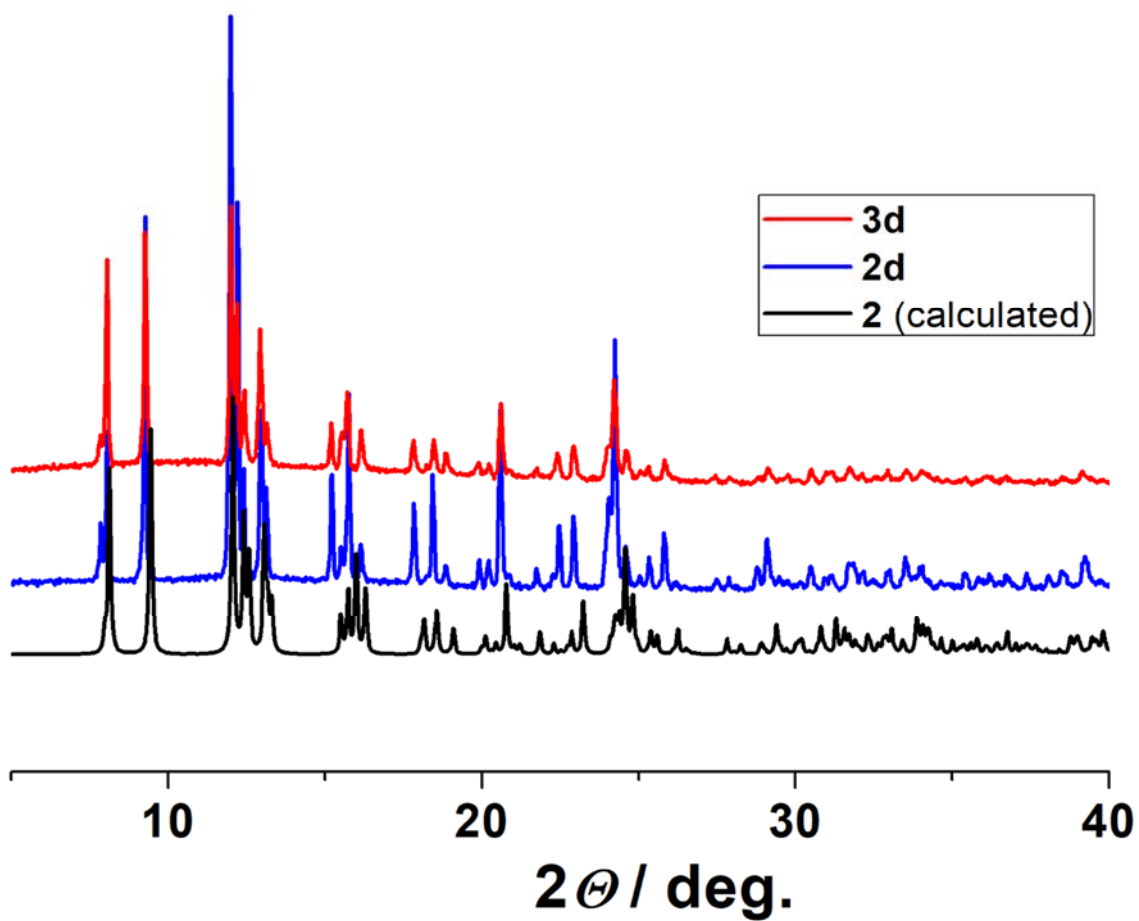


Fig. S1. Powder X-Ray spectra for the diluted complexes **2d** and **3d**. In black is represented the simulated powder spectra from the single crystal structure of the complex **2**.

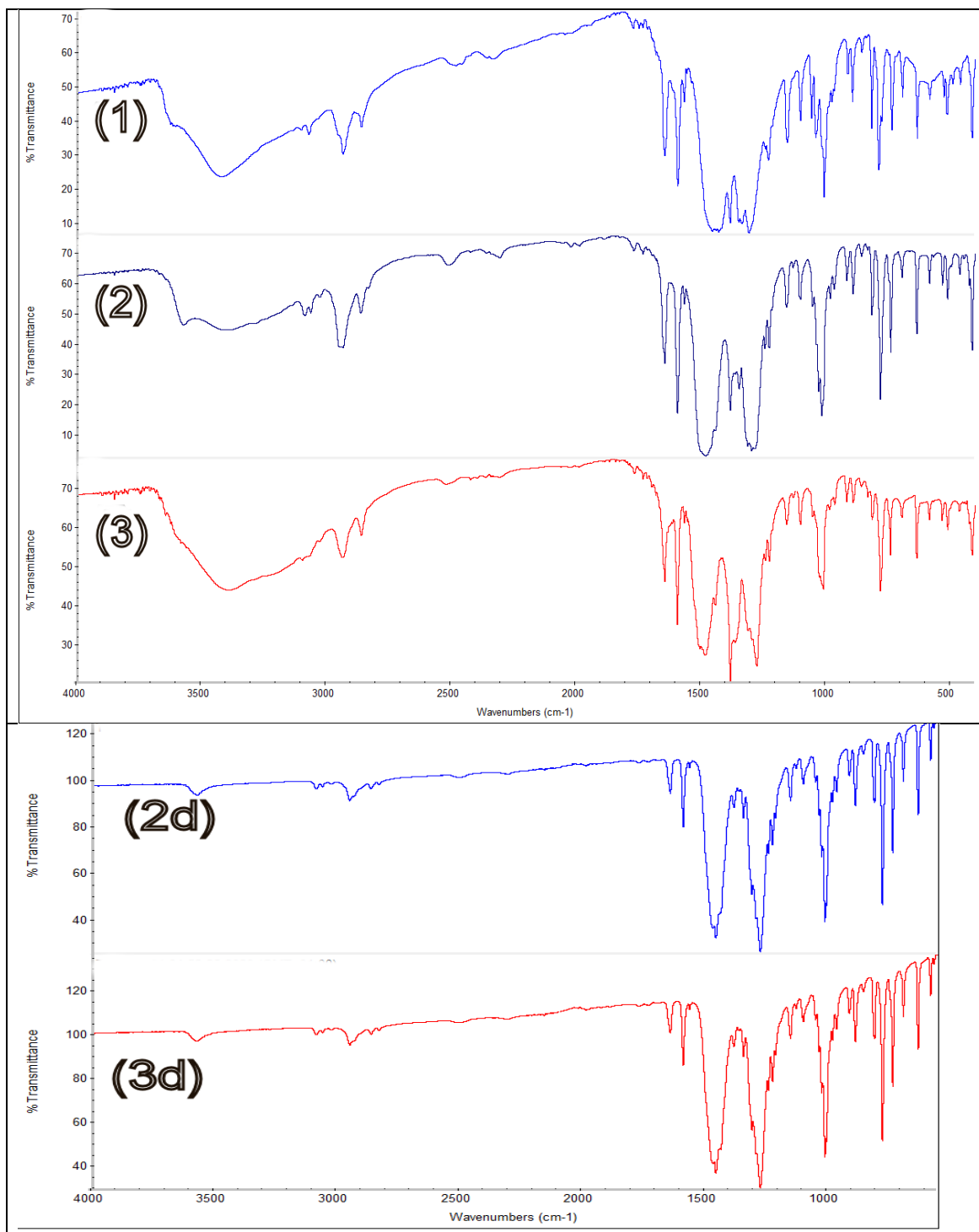


Fig. S2. IR spectra for complexes [Ce(L)(NO₃)₃(MeOH)] (1), [Gd(L)(NO₃)₃] (2) and [Dy(L)(NO₃)₃] (3) the diluted 2d and 3d.

Table S1. CShM values for the undecacoordinated environment of complex **1** and the decacoordinated complex **2**. The relatively high distortion with the ideal polyhedra are due to the low bite of the nitrate and *cis* N-donors of the Schiff base.

11-vertex Polyhedra	Ce ^{III} (1)	10-vertex Polyhedra	Gd ^{III} (2)
Capped pentagonal prism (C5v)	5.64	Bicapped cube (D4h)	9.77
Capped pentagonal antiprism (C5v)	5.99	Bicapped square antiprism (D4d)	4.67
Augmented sphenocorona (cs)	7.73	Metabidiminshed icosahedron (C2v)	7.08
		Sphenocorona (C2v)	3.05
		Staggered Dodecahedron (D2)	4.66

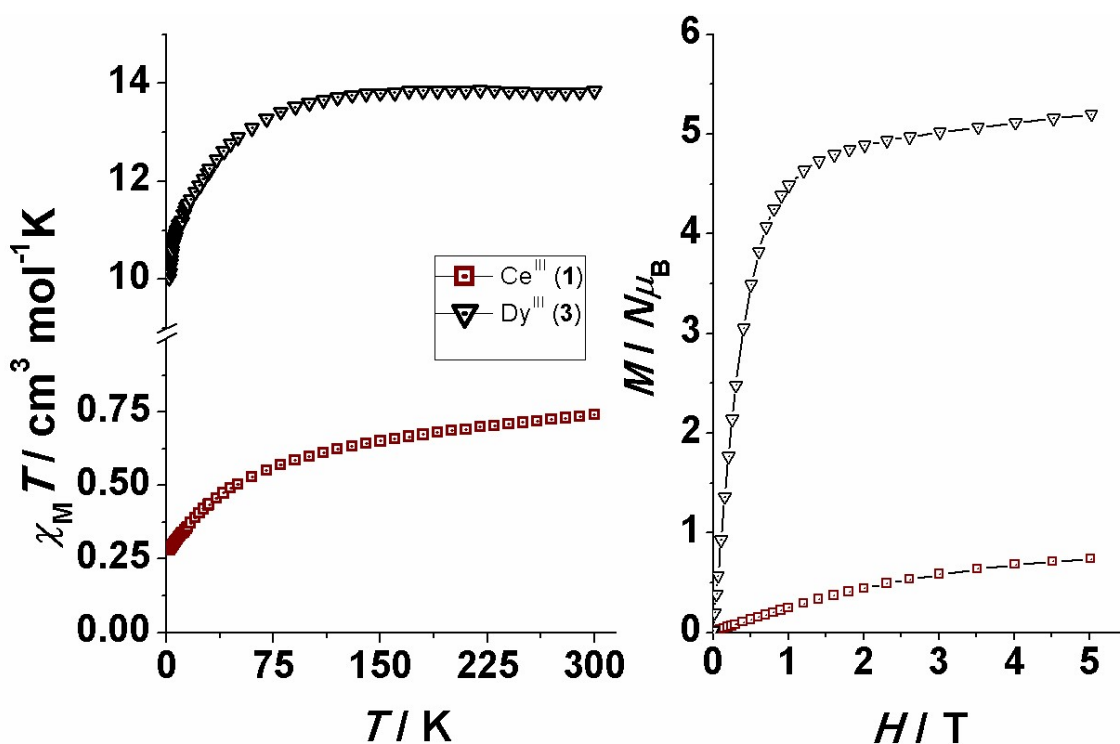


Fig. S3. $\chi_M T$ (left) and magnetization (right) plots for referred complexes. The $\chi_M T$ values at room temperature are very close to the expected values for a lonely isolated lanthanide ions (**expected/experimental** $\text{cm}^3 \cdot \text{mol}^{-1} \cdot \text{K}$): Ce^{III}, (${}^2F_{5/2}$, $g = 6/7$, **0.80/0.74** $\text{cm}^3 \cdot \text{mol}^{-1} \cdot \text{K}$), Dy^{III} (${}^6H_{15/2}$, $g = 4/3$, **14.2/13.8** $\text{cm}^3 \cdot \text{mol}^{-1} \cdot \text{K}$).

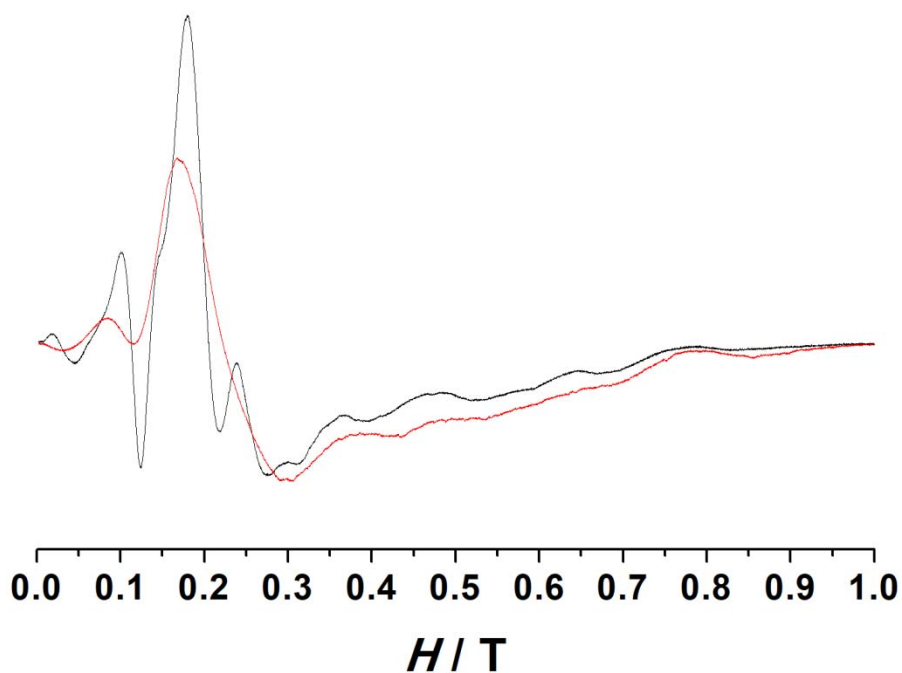


Fig. S4. X-band EPR spectra for the Gd^{III} compounds **2** (red) and **2d** (black). Reduction of dipolar interactions allows sharper lines for **2d**. The identical spectra confirm the same environment after dilution.

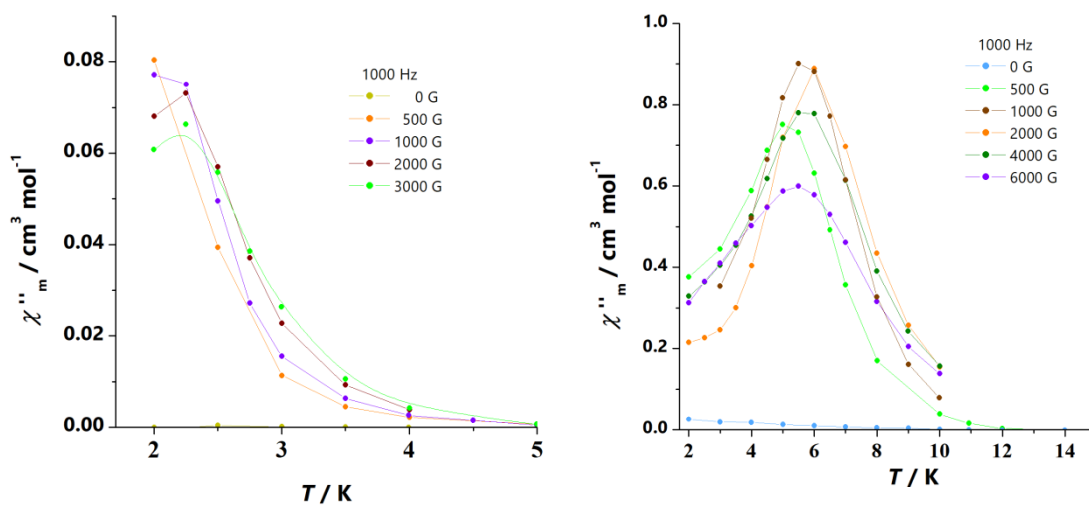


Fig. S5. χ''_m dependence of the transverse field for complex **1** (left) and **3** (right). From this initial dependence the fields to perform the *ac* measurements were 2000 G for **1** and 1000 G for **3**.

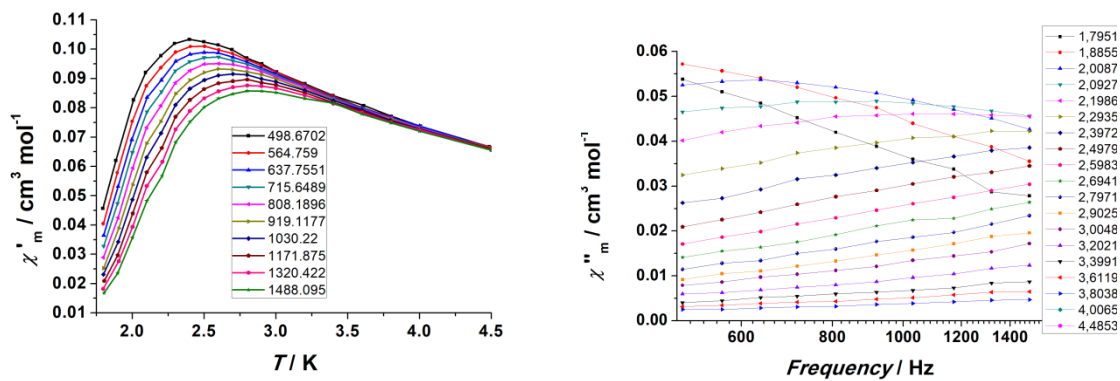


Fig. S6. χ'_M vs. T (left) and χ''_M vs. frequency (right) for complex **1**.

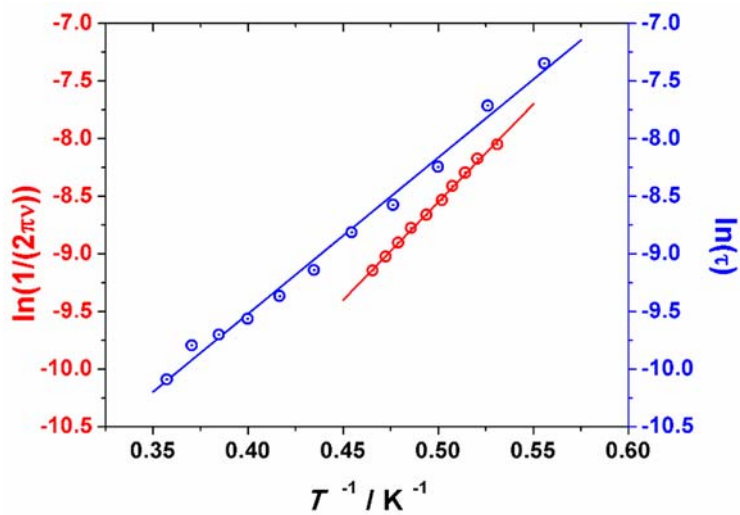


Fig. S7. Plot of $\ln(1/2\pi\nu)$ vs. T^{-1} from the $\chi''_M(T)$ data (red) and $\ln(\tau)$ vs. T^{-1} from the fit of the Argand plot (blue) for complex **1**.